SUPPRESSION OF BIODYNAMIC INTERFERENCE

BY ADAPTIVE FILTERING

by

M. Velger, S.J. Merhav and A.J. Grunwald

Department of Aeronautical Engineering
Technion - Israel Institute of Technology
Haifa 32000, Israel

ABSTRACT

A novel approach for suppressing biodynamic interference by means of adaptive filtering, is described. Preliminary experimental results obtained in moving base simulator tests are presented. Both for pursuit and compensatory tracking tasks, a strong deterioration in tracking performance due to biodynamic interference is found. The use of adaptive filtering is shown to substantially alleviate these effects, resulting in a markedly improved tracking performance and reduction in task difficulty. The effect of simulator motion and of adaptive filtering on Human Operator describing functions is investigated. Adaptive filtering is found to substantially increase pilot gain and cross-over frequency, implying a more "tight" tracking behaviour. The adaptive filter is found to be effective in particular for high-gain proportional dynamics, low display forcing function power and for pursuit tracking task configurations.

I. INTRODUCTION

Biodynamic interference is a bothersome problem in the man-machine systems area. It occurs when a manual control task is performed on a platform, subjected to translatory or angular external accelerations. Typical examples are: the manual control of large flexible aircraft flying through strong convective turbulence, the manoeuvering of fighters under transonic buffeting conditions, tracking tasks performed on hovering rotorcraft, high-speed vehicles travelling over rough terrain or waves, etc. [1-3]. In such tasks the manual control performance may be severely impaired by the resulting involuntary pilot control commands. These originate in the biomechanical coupling between the vibrating vehicle and the control manipulator ("stick feedthrough"), which may be either manual or head mounted, such as in helmet sights. This coupling is due to the dynamic response of various human body elements to external accelerations. In addition to the direct additive stick feedthrough, the vibration of limbs and head increases the pilot remnant noise level, either by interfering with neuromuscular feedbacks needed for precise manual control, or by degrading the visual acuity due to the relative motion between the eye point-of-regard and the display, causing image blurring, [4].

Although the severe effects of biodynamic interference on the pilot vehicle system have been recognized [1-3], successful efforts to eliminate these interferences have so far not been reported. The approach attempted has been to mechanically isolate the pilot from the aircraft by passive means, such as shock-absorbing seats, armrests, etc., [5,6] or by active isolation systems e.g.

Active Vibration Isolation Systems (AVIS), [7,8]. However, since these methods reduce the pilot's inertial accelerations, they actually increase his motion relative to the display or manipulator. Consequently no significant performance improvement was obtained [8]. Moreover, vibration isolation may be undesirable since it may impair the pilot's "seat of the pants" motion cues.

In this paper an adaptive disturbance cancellation technique to eliminate the involuntary pilot commands is described. A Least Mean Square (LMS) adaptive filter [9] has been employed. Its main advantage is its inherent ability to automatically adjust its parameters so that its design requires little or no a priori knowledge of input or human response characteristics. The adaptive filter utilizes the measurements of a platform mounted accelerometer to generate a signal which is a close estimate of the involuntary pilot command. This signal is subtracted from the stick output, thus largely cancelling the biodynamic interference. Since the adaptive algorithm requires little computational effort and memory, it can be easily implemented by a low cost microprocessor.

II. PRINCIPLE OF OPERATION

The following two major cases are considered:

1. The "biodynamic open loop" case, in which the platform motions are independent of the manipulator forcing function. Examples are: pointing of sights or weapons on a moving ship deck or helicopter.

2. The "biodynamic closed loop case" in which the platform motions partly result from the control stick command itself, such as the piloting of an aircraft. The resulting biodynamic stick feedthrough again causes a platform motion, thus constituting a circulating signal.

A block diagram of the biodynamic "open loop" case is shown in Fig. 1. The control error ε between the desired reference signal c and the actual response r is presented to the Human Operator (HO) on a display monitor as the displayed error ε_d. This signal is utilized by the HO to generate the voluntary control command u_c. On the other hand, the biodynamic interference due to the platform motions, generates an involuntary control command u_b which is added to u_c resulting in a total control command u_t. This command being either the control stick force or displacement is translated into an analog or digital signal u. The platform motions are measured by a platform mounted accelerometer. Its output a is passed through a high-pass filter in order to block low-frequency motion components which should not be subtracted. The filtered signal is applied to the adaptive filter and causes it to generate the signal u_a, which is a least squares estimate of the additive interference u_b. By subtracting u_a from u, the filtered control command u_f is obtained.

The diagram of the biodynamic "closed-loop" case is shown in Fig. 2. Unlike the biodynamic open loop case, the aircraft response constitutes the motion disturbance. Therefore, the input to the adaptive filter is now dependent on the voluntary command u_c, which causes a bias in the estimation of u_b. This difficulty can largely be overcome by the use of the high-pass filter, which separates the aircraft response to desired control, which is basically of low frequency, from the aircraft response to involuntary biodynamic disturbance, which is basically of high frequency. The feasibility of this approach has been

demonstrated by digital simulations in Ref. [10]. An example is given of a YF-12 aircraft, in which the stick feedthrough in the longitudinal axis of control results in diverging pilot induced oscillations. The adaptive filter is able to suppress these oscillations effectively without affecting the dynamic response of the aircraft.

In this paper only the biodynamic "open loop" case is evaluated experimentally. The biodynamic "closed loop" case is a subject for further study.

III. EXPERIMENTAL PROGRAM

A. Objectives of the Experiments

The objectives of the experiments were: 1) To investigate the effect of motion on tracking performance in various tasks and 2) to evaluate the effectiveness of the adaptive filter in reducing the effects of biodynamic interference. For this purpose the variances of tracking error and control command were computed and separated into three components: 1) A component correlated with the tracking task forcing function, 2) a component correlated with the simulator motions and 3) a residual uncorrelated component due to pilot remnant. Futhermore, in order to achieve better insights of cause and effect in the error and control signals components, the visual motor dynamic response properties of the human operator were analyzed and computed. In these computations the auto and cross power spectral density functions were computed first and used to determine pilot control and biodynamic transfer functions as well as tracking error and control variance components.

B. Experimental Set-Up

The experimental set-up is shown in Fig. 3. The dynamical tests were carried out with a three-degree-of-freedom moving-base simulator, designed and built at the Flight Control Laboratory at the Technion, Haifa, Israel. The simulator cabin is suspended from three rods, each of which can be moved up and down independently by separate DC torque motors. By moving the rods either collectively or differentially, heave, pitch and roll, or combinations thereof, can be generated. The total weight of the cabin and the subject is balanced by a pneumatic system consisting of an air bellow connected to a large pressure tank. The platform motions are generated digitally in real-time by a DGC Nova 3 minicomputer. The computed motions are converted into analog signals which are fed into the controllers and power amplifiers which drive the torque motors to obtain the required motion. The cabin includes (1) an aircraft ejection seat with automobile type cushions and seat belt; (2) a two-axis isomorphic side stick of an F-16 aircraft; (3) a 9 inch TV monitor on which the tracking task is displayed, and (4) a package of accelerometers and rate gyros, measuring the platform motions. The measured analog signals of the pilot's total control output consisting of voluntary and involuntary control commands as well as platform accelerations, are converted into digital signals and fed into the Nova computer. The computer implements the adaptive filter in real-time and simulates the motions of the controlled element as well as its forcing function. These computed motions are converted into analog signals, fed into a display generator and visualized on the TV monitor in the simulator cabin. During the test run

control commands, controlled element motions as well as platform motions, are recorded and stored on a 10 megabyte disk for further off-line processing.

C. Description of the Experiments

Two tracking tasks were performed in the experiments: 1) A compensatory task, representing e.g. a missile, remotely guided by a vehicle mounted TV camera and 2) a pursuit task representing a teleoperated electro-optical device. For each experimental configuration three cases were investigated. In the first case the tracking task was performed in the absence of motion (static case S), in the second case motion was present but the adaptive filter was not activated (case M) and in the third case motion was present and the adaptive filter was activated (case A). The duration of each test run was 245 seconds during which time histories of the various signals were recorded. For each experimental configuration, each of the cases S,M and A were repeated at least three times in a random sequence, unknown to the subject.

In the experimental program both the display forcing function power and the dynamics of the controlled element were parameters. Their effect on performance and effectiveness of the adaptive filter was investigated.

D. Description of the Tracking Tasks

Both in the compensatory and in the pursuit tracking task the controlled element dynamics included a pure integration combined with a proportional part. This choice was made in order to investigate the biodynamic effects and effectiveness of the adaptive filter in the basic rate and position control tasks. The transfer function of the controlled element is given by:

$$\frac{r(s)}{u_f(s)} = K \cdot \left\{ \frac{1}{s} + K_p \cdot \frac{\omega_o^2}{(s^2 + 2\xi\omega_o s + \omega_o^2)} \right\} \tag{1}$$

The second order filtering of the proportional part was included to avoid the appearance of rapid, high frequency display motions. The filter natural frequency ω_o was set to 15 rad/sec and the damping ratio ξ was set to 0.707. The tracking tasks were performed in two axes of control, where for each axis the dynamics of Eq. (1) was employed. However, the adaptive filter was implemented in the lateral axis of control only. On the display monitor a cross and a square were shown. In the compensatory task the cross was kept fixed in the center of the screen and symbolized the controlled element vehicle axis. The square symbolized the target as seen through a vehicle mounted TV camera, and the target motions c were generated for each axis of control independently by passing bandlimited zero-mean Gaussian white noise processes through second order filters with $\omega_o = 0.7$ rad/sec and $\xi = 0.3$. Thus the deviations of the square from the cross at the center of the screen represented the displayed tracking error ε_d between target motion c and controlled element response r. The objective of the task was to minimize ε_d by bringing the square to the cross center. In the pursuit task the cross symbolized the controlled element and the square the target, as seen both through a platform mounted optical device. In contrast to the compensatory task, the cross deviated from the screen center, where the deviations corresponded to the controlled element response r. The motions of the square symbolized the target motions c, which were generated by the same forcing functions

as for the compensatory task. Also in the pursuit task the objective was to reduce the error ε_d in the attempt to maintain coincidence of cross center and square.

The stick gearing was the same for both axis. For the compensatory task it was set at 1.24 N/cm and for the pursuit task at 0.79 N/cm.

E. Description of the Simulator Motions

The lateral accelerations were obtained by a roll-motion of the simulator cabin. The simulator motions were generated by passing bandlimited zero-mean Gaussian white noise through a second-order filter with $\omega_0 = 15$ rad/sec and $\xi = 0.707$. This signal constituted the roll-angle command imparted to the controllers of the simulator. The power spectrum of the actual measured lateral accelerations is shown in Fig. 4. The notch at about 3 rad/sec is inherent to the pendulum type suspension of the simulator. The RMS value of the lateral accelerations was measured to be 0.24g.

F. Subject Background and Training

Four subjects participated in the experimental programs. Subject B was female. Only subject D had actual flight experience as a military helicopter pilot. Subjects B and D were Aeronautical Engineering students and A and C Aeronautical Engineers. Subjects A and B had extensive prior fixed base simulator training.

Each simulation session lasted one hour. An average of 5 training hours was required for the subjects to reach a stable level of performance. Only the results of subject A are presented in this paper. However, very similar trends in the results of the other subjects were noticed.

G. Experimental Results

The values of the display forcing function power σ_{in} and of the controlled element proportional gain K_p, for the various configurations, are listed in Table 1. The experimental results for subject A are summarized in Figs. 5-11.

Configuration	Tracking Task C-compensatory P-pursuit	Display Forcing Function Power σ_{in} [mm]	Proportional Gain K_p
I	C	7.8	0.022
II	C	15.5	0.022
III	C	31	0.022
IV	C	15.5	0.2
V	P	15.5	0.022
VI	P	15.5	0.2

Table 1: Tracking Task Parameters.

1. Tracking Performance in the Presence of Motion

The variance components of the error and of the stick output are shown in Figs. 5-7. Fig. 5 shows that for all compensatory tracking configurations the total variance in the presence of motion (M) is markedly larger than the variance for the static case (S). For all configurations the vibration correlated component constitutes a considerable part of the total error variance. Fig. 6 shows components of the total stick output u, i.e. voluntary command u_c plus stick feedthrough u_b. Also the total stick output in the presence of motion (M) is markedly larger than in the static case (S). For all cases the vibration correlated component of the stick output variance caused by stick feedthrough, is dominant. The input correlated component is the second largest and the remnant component is the smallest. Fig. 7 shows that for pursuit tracking, the effect of the stick feedthrough on error and on stick output is even larger than for compensatory control. Both for compensatory and for pursuit tracking a marked increase in remnant between the static case (S) and the motion case (M) is noticed. The subjects commented that tracking in the presence of motion was considerably more straining and difficult to perform.

2. Tracking Performance with the Adaptive Filter

Fig. 5 shows for all configurations a substantial reduction in the total error variance as a result of the incorporation of the adaptive filter, case A. This improvement with respect to case M is mainly due to a marked reduction in the vibration correlated component of the error variance and, to a lesser extent, to a reduction in the input correlated components. This indicates that the suppression of stick feedthrough also improves the ability to track the forcing function. On the other hand the remnant component generally increases slightly. Fig. 6 shows that also for the adaptive filter the vibration correlated component of the total unfiltered stick output u is considerably large (case A) though smaller than without the adaptive filter (case M). However, for the filtered output u_f (case A) the vibration correlated component is very small. Fig. 7 shows similar trends of the effect of the adaptive filter for pursuit tracking.

The effectiveness of the adaptive filter is demonstrated by time-histories shown in Figs. 8 and 9. Fig. 8 shows the stick output and adaptive filter output in the presence of motion while the display forcing function was set to zero, i.e. $\sigma_{in}=0$. In this case the control output is almost entirely due to stick feedthrough. Fig. 8 shows that the adaptive filter output signal closely "copies" the stick feedthrough signal and that the difference between them, being u_f, is small.

Time histories for a second example with $\sigma_{in} = 15.5$ mm are shown in Fig. 9. The tracking error in the dynamic case (M) is considerably larger than in the static case (S). The tracking error in the presence of the adaptive filter (A) is much smaller than in the dynamic case (M) and only slightly larger than in the static case (S).

The subjects commented that tracking in the presence of the adaptive filter was considerably easier than without the filter, and that the filter enabled them to improve their tracking accuracy.

3. The Effect of Display Forcing Function Power

Fig. 5 shows, as can be expected, that for a small forcing function power σ_{in}, the vibration correlated component of the error is more dominant than for

high power. Hence, for low forcing function power, the adaptive noise cancellation is more pronounced and therefore relatively more effective.

4. Effect of the Controlled Element Proportional Gain

Fig. 5 shows that an increase in proportional gain has no significant effect on the error score in the static case, (see (S) of configurations II and IV). However, in the presence of motion the total error for high-proportional gain is markedly larger than for low-proportional gain (see case M of configurations II and IV). This is mainly due to the larger effect of stick feedthrough. The incorporation of the adaptive filter strongly reduced the stick feedthrough as well as the input correlated component of the error and thus strongly improved tracking accuracy, (see case A of configurations II and IV). Therefore, for tasks with high proportional gain, it is indicated that the adaptive filter is particularly effective. A similar, but even more pronounced trend was found for pursuit tracking, see configurations V and VI in Fig. 7.

5. Effect of Motion and Adaptive Filtering on Human Operator Response

Figs. 10 and 11 show the visual motor dynamic response properties, characterized by open loop transfer function cross-over frequency and phase margin, and low-frequency pilot and biodynamic gains. For all configurations it is shown that motion (M) strongly reduces the cross-over frequency and pilot gain and increases the phase margin as compared to the static case (S). This indicates that in the presence of biodynamic interference the tracking response is more inhibitive, a fact which is confirmed by the subjects. The adaptive filter causes an increase in cross-over frequency and pilot gain and a reduction in phase margin, see (A) in Figs. 10 and 11. It should be noted that the cross-over frequency and phase margin with the adaptive filter are close in value to those of the static case. In most cases the cross-over frequency even exceeds the one of the static case and the phase margin is correspondingly smaller. This indicates that with the adaptive filter the tracking behaviour is more "tight". Consequently the low-frequency gain of the biodynamic feedthrough is considerably larger for the adaptive filter than without it, as can be seen from Figs. 10 and 11). This implies that with the adaptive filter the subject allows himself a firmer grip on the control stick, as compared to case M without the filter, in which he   tends to release his grip in order to alleviate the stick feedthrough effects. This fact was also confirmed by the subjects.

6. Motion Cross-Talk

Finally it should be noted that the adaptive filter was employed in the lateral axis of control only. However, due to cross-talk effects in the simulator motion and biodynamic response, part of the interference appeared in the vertical axis of control as well. Since these disturbances were not filtered the vertical error was considerably larger than the lateral one. It is anticipated that a reduction in the vertical error by employing an adaptive filter in both axes of control, will improve the lateral tracking performance even more.

IV. CONCLUSIONS

1. For the configurations considered, lateral accelerations seriously impair tracking performance as a result of biodynamic interference.

2. Apart from the error component caused by stick feedthrough, the biodynamic interference increases the input correlated and remnant components of the error and strongly increases the task difficulty.

3. The biodynamic interference reduces the cross-over frequency and low-frequency pilot gain, implying a more inhibited tracking strategy.

4. Performance deterioration due to stick feedthrough is the strongest for high proportional gain dynamics and low tracking forcing function power.

5. The adaptive filter markedly reduces the total tracking error by reducing the vibration and input correlated components of the error and thus substantially reduces task difficulty.

6. The adaptive filter is effective in particular for high proportional gain dynamics, low display forcing function power and in the pursuit tracking configurations.

7. The adaptive filter causes a substantial increase in cross-over frequency and pilot gain and reduces the phase margin implying a more "tight" tracking behaviour.

8. The adaptive filter yields an increased biodynamic low-frequency gain and slightly increased remnant which indicates that the subject's grip of the control stick is firmer.

9. It is anticipated that even for single-axis motion excitation it is desirable to employ an adaptive filter in both axes of control.

V. ACKNOWLEDGEMENTS

VI. REFERENCES

1. Jex, H.R., Evaluating Biodynamic Interference with Operation Crews, Vibration and Combined Stresses in Advanced Systems, AGARD CP-145, pp. B24-1-B24-18.

2. Jex, H.R., Problems in Modeling Man Machine Control Behavior in Biodynamic Environments, Proc. 7th Annual Conf. on Manual Control, NASA SP-281, 1971.

3. Jex, H.R. and Magdaleno, R.E., Progress in Measurement and Modeling the Effects of Low Frequency Vibration on Performance, AGARD CP-253, March 1980.

4. Levison, W.H., Model for Human Controller Performance in Vibration Environments, Aviat. Space and Environ. Med. 49:321-327, Jan. 1978.

5. Jex, H.R. and Magdaleno, R.E., Biomechanical Models for Vibration Feedthrough to Hands and Head for a Semisupine Pilot, Aviat. Space and Environ. Med. 49: 304-316, Jan. 1978.

6. Levison, W.H. and Houck, P.D., Guide for the Design of Control Sticks in Vibration Environments, AMRL-TR-74-127, Aerospace Medical Research Laboratory, Wright Patterson AFB, Oh. 1975.

7. Schubert, D.W., Pepi, J.S. and Roman, F.E., Investigation of the Vibration Isolation of Commercial Jet Transport Pilots During Turbulent Air Penetration, NASA CR-1560, July 1970.

8. DiMasi, F.P., Allen, R.F. and Calcaterra, P.C., Effect of Vertical Active Vibration Isolation on Tracking Performance and on Ride Qualities, NASA CR-2146.

9. Widrow, B. et al., Adaptive Noise Cancelling: Principles and Applications, Proc. IEEE, Vol. 63, No. 12, December 1975, pp. 1692-1716.

10. Velger, M., Grunwald, A. and Merhav, S., Suppression of Biodynamic Disturbances and Pilot Induced Oscillations by Adaptive Filtering, 25th Israel Annual Conference on Aviation and Astronautics, Feb. 23-25, 1983, pp. 45-54.
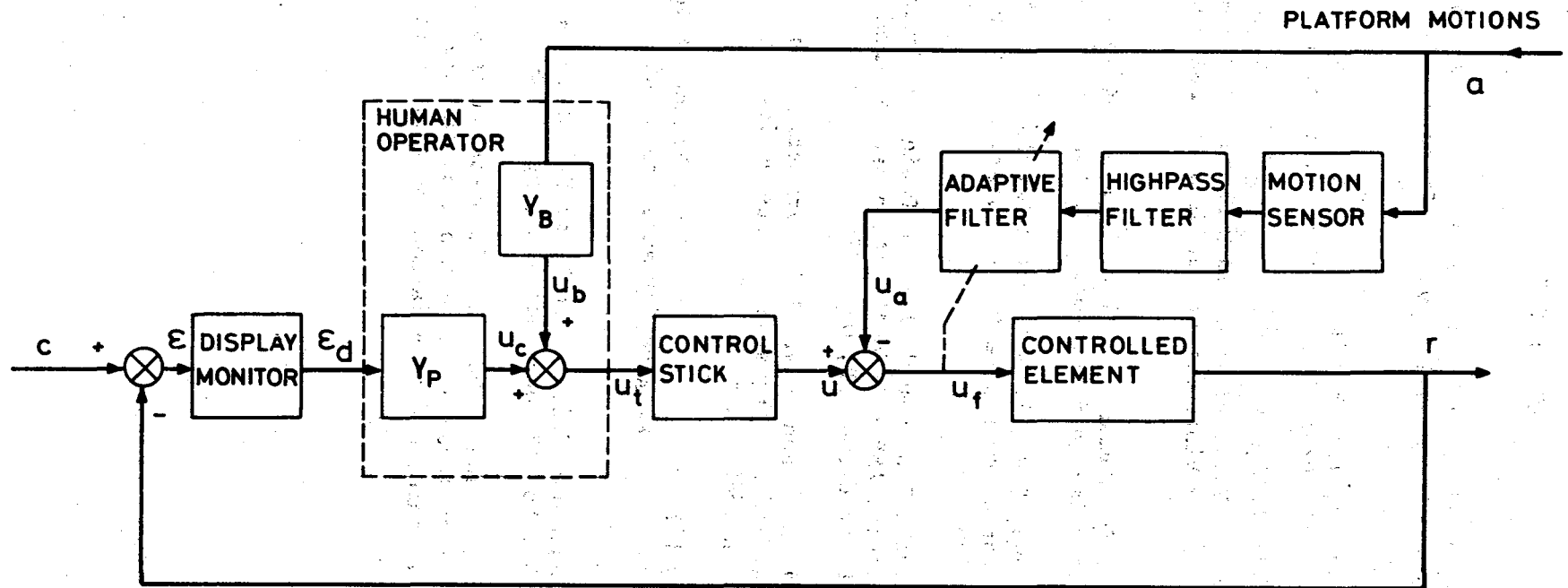
Figure 1. Adaptive Filtering scheme of Biodynamic Interference in Manipulation Tasks (Biodynamic "Open Loop" Case).
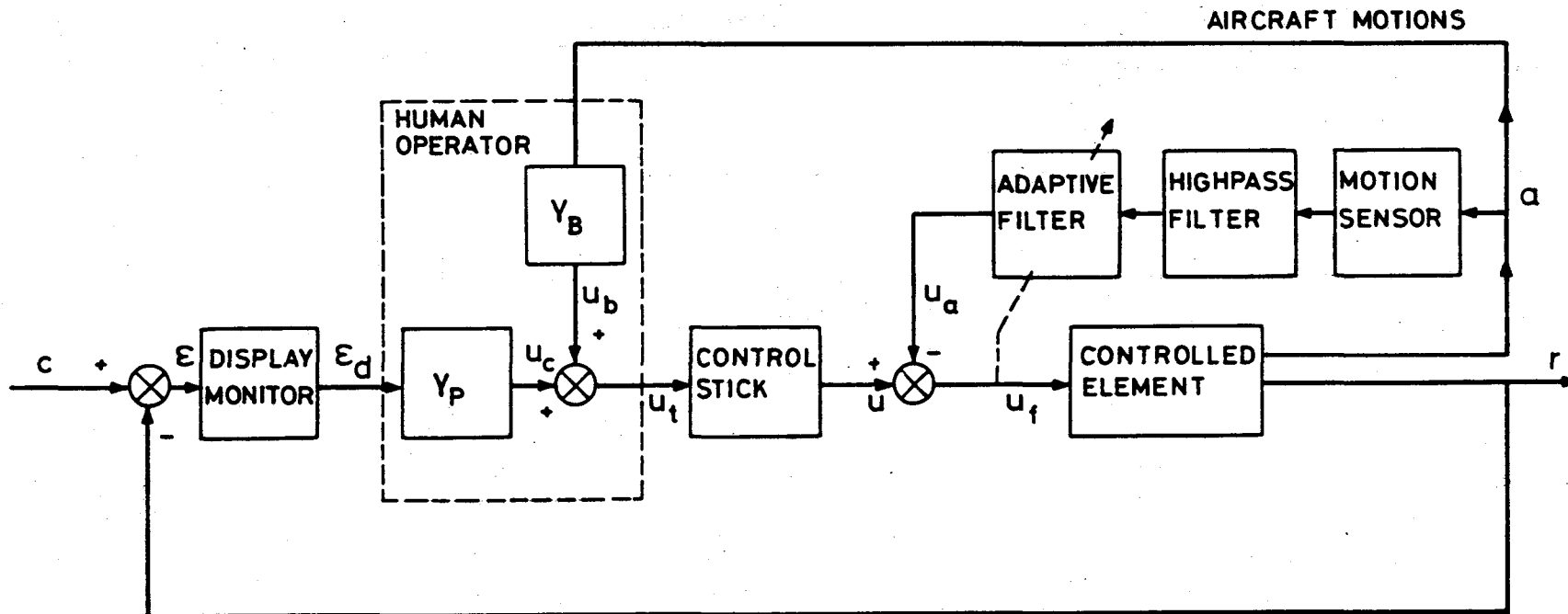
708

Figure 2. Adaptive Filtering Scheme of Biodynamic Interference in
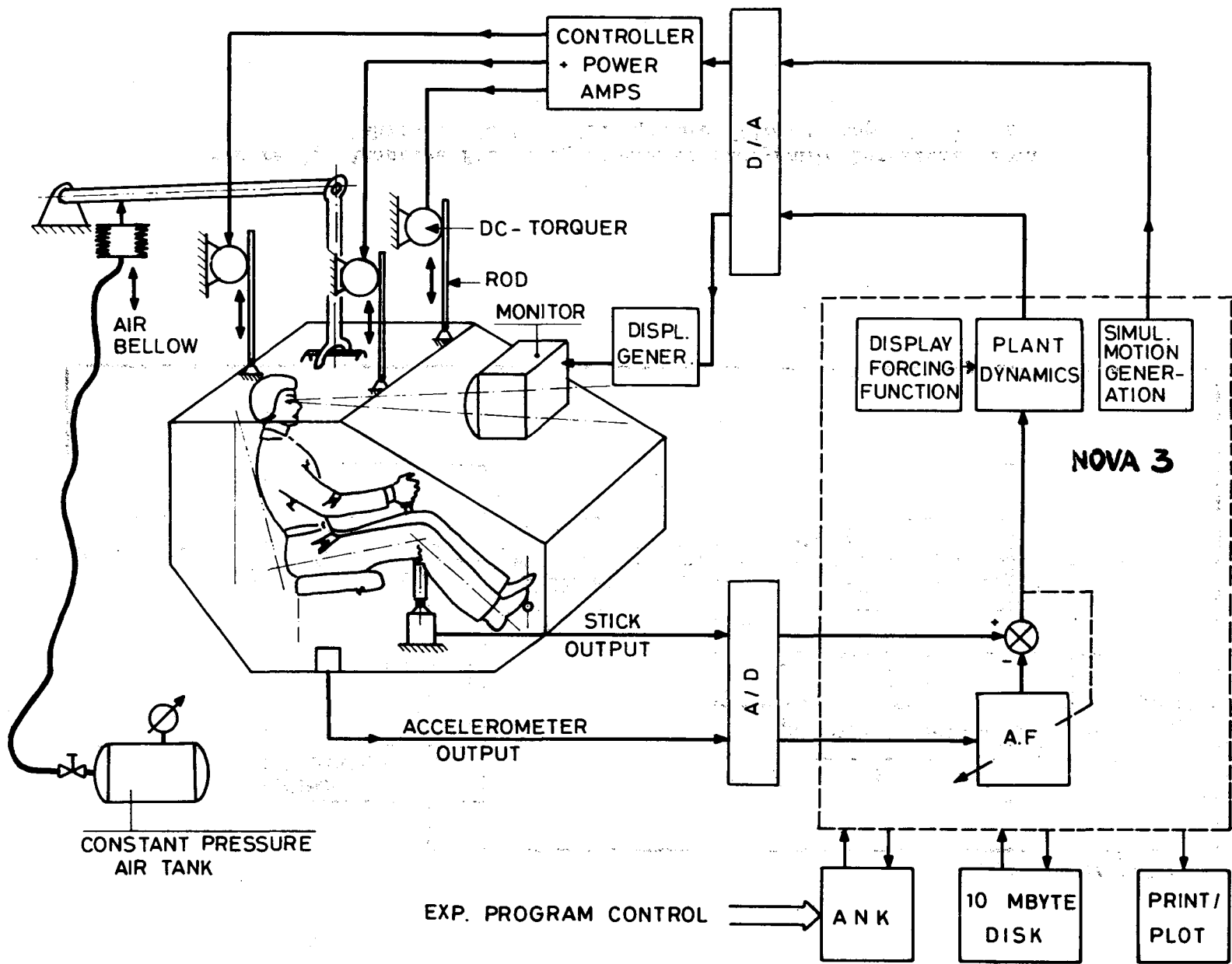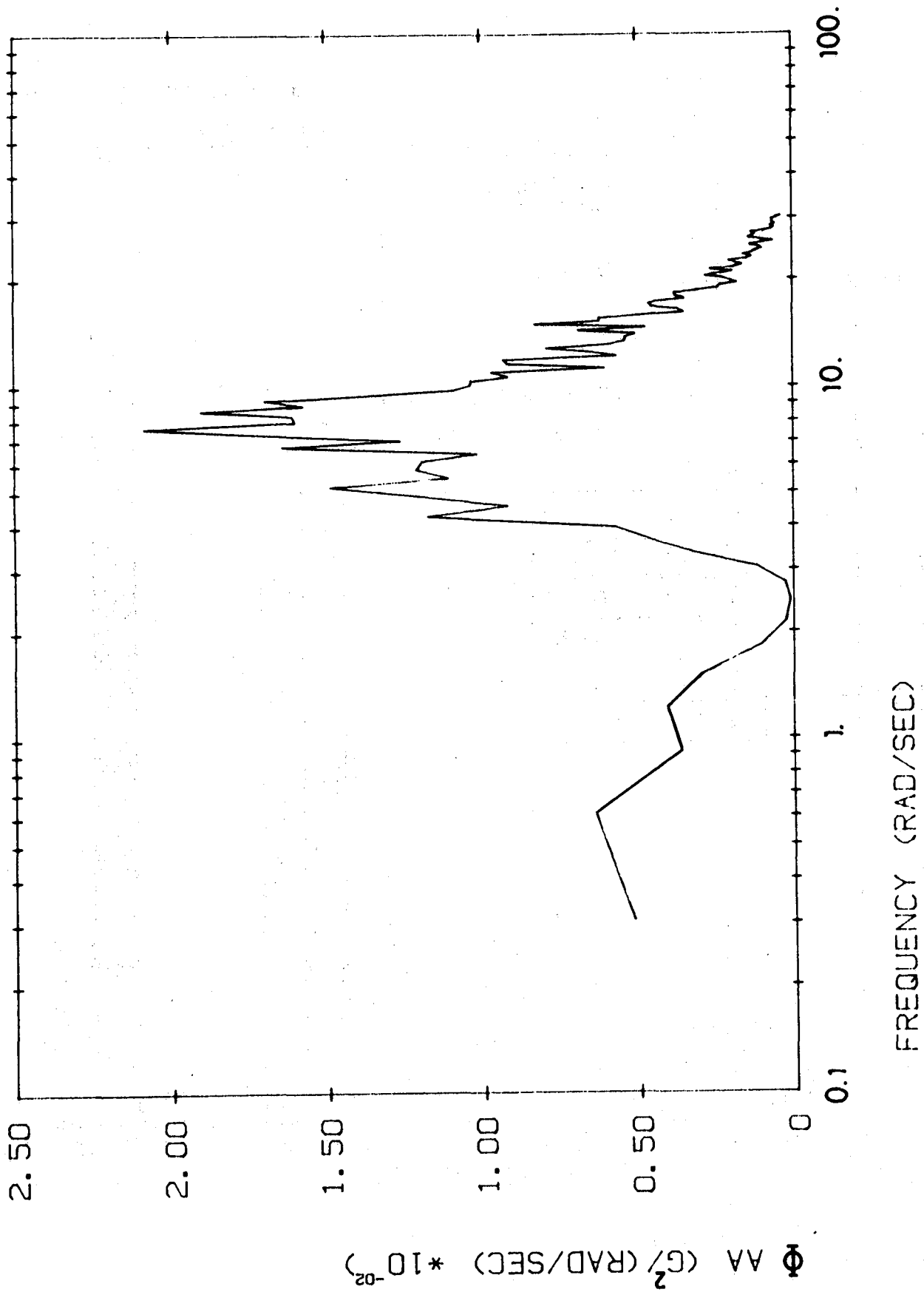Vehicular Control (Biodynamic "Closed Loop" Case).

Figure 3. Experimental Setup.

Figure 4. Power Spectrum of Lateral Simulator Accelerations.

FREQUENCY (RAD/SEC)

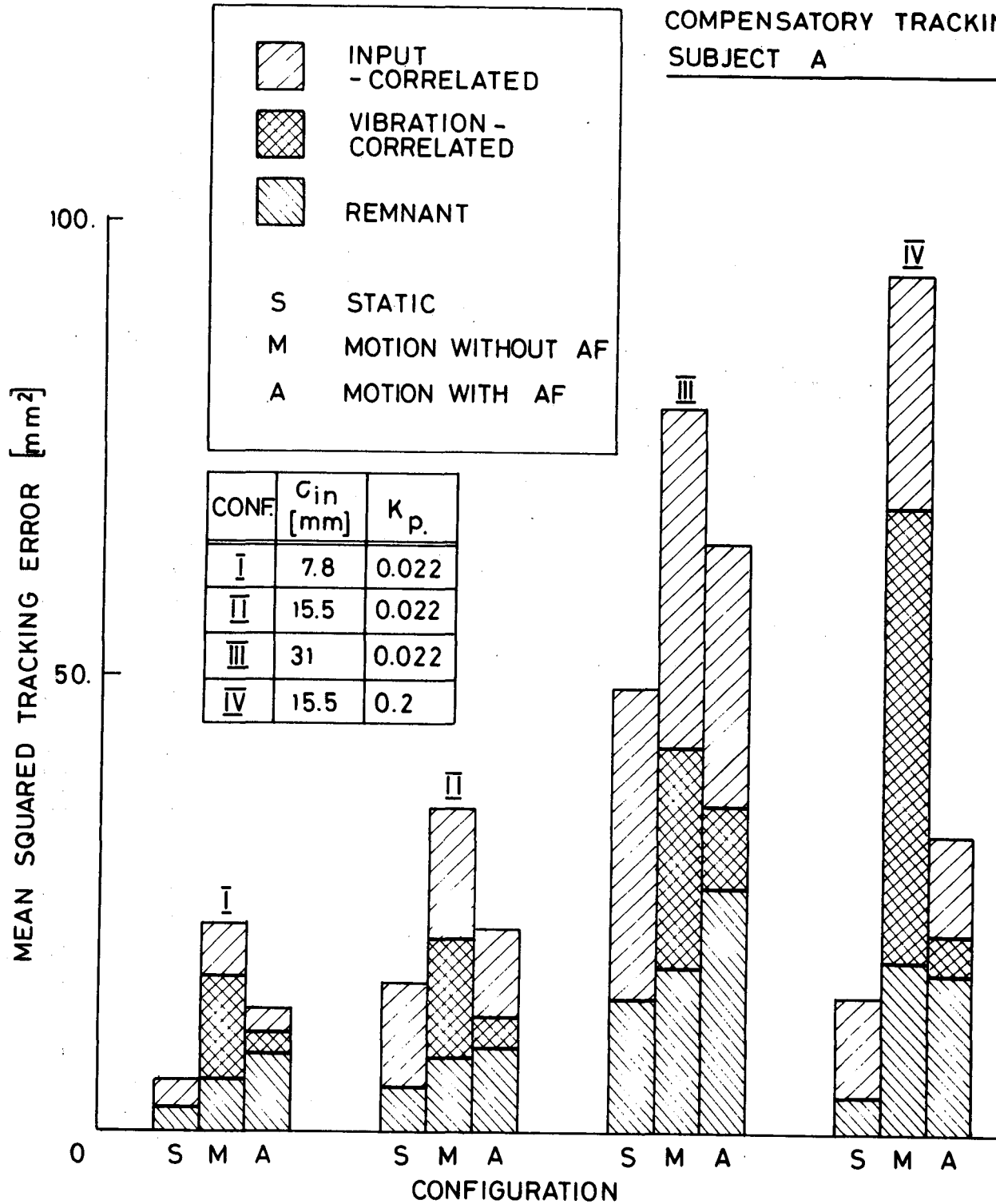Φ AA $(G^2/(RAD/SEC) *10^{-02})$

Figure 5. Variance Components of the Tracking Error for the
Compensatory Task; Subject A.

712

CONF.	C_{in} [mm]	K_P
I	7.8	0.022
II	15.5	0.022
III	31	0.022
IV	15.5	0.2

COMPENSATORY TRACKING
SUBJECT A
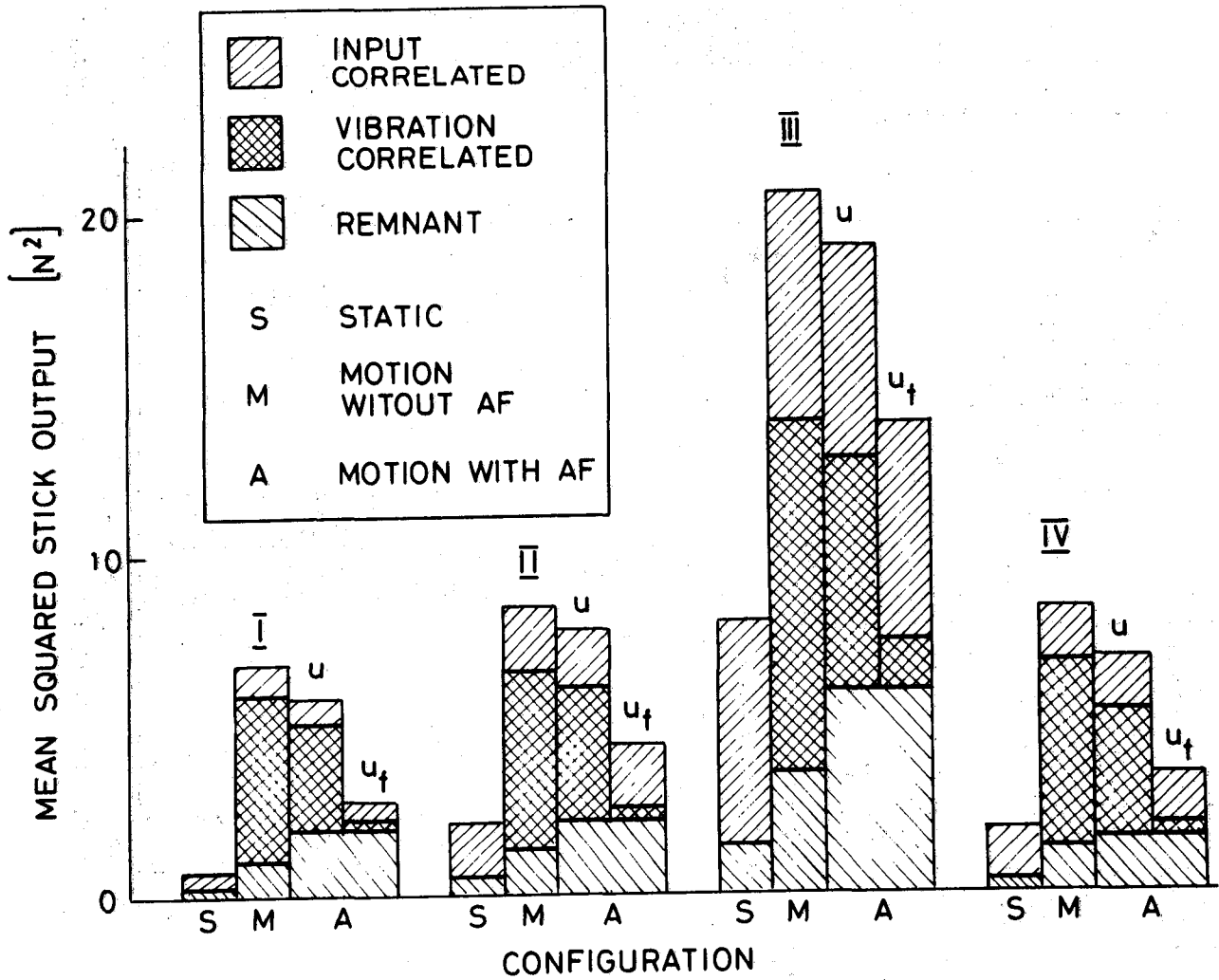
Figure 6. Variance Components of the Stick Output for the Compensatory Task; Subject A.

713
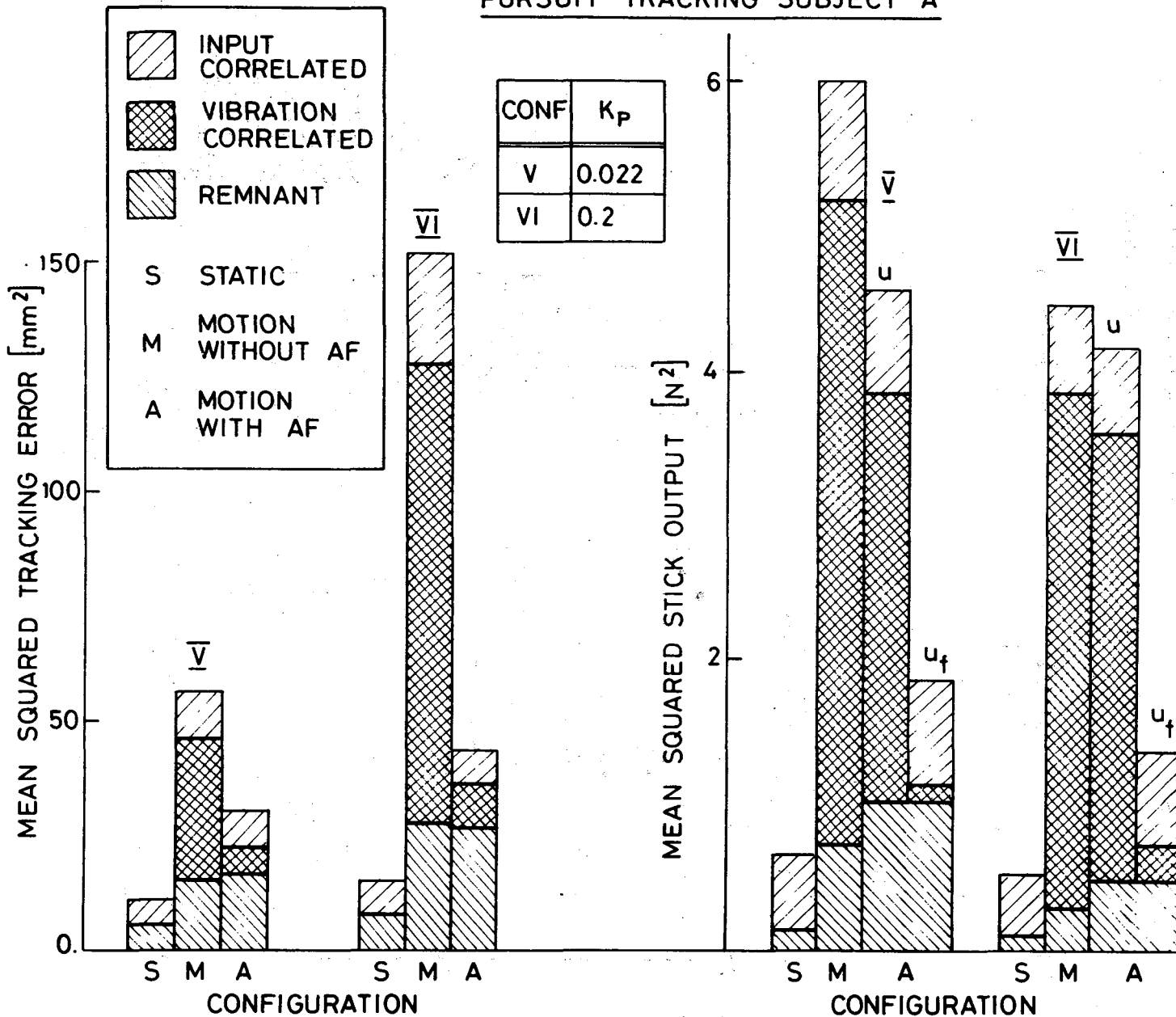
Figure 7. Variance Components of the Tracking Error and
Stick Output for the Pursuit Task; Subject A.
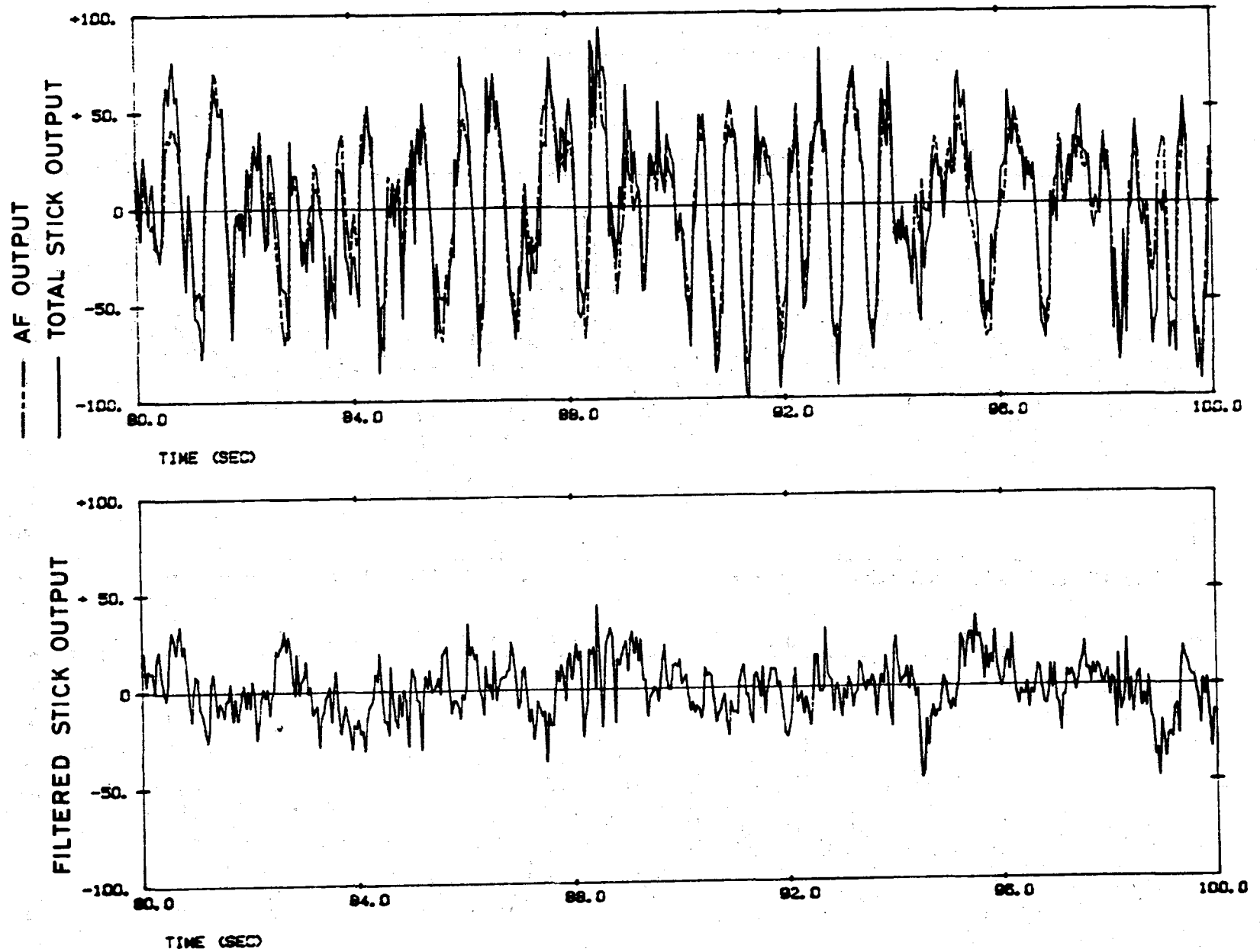
Figure 8. Time-Histories of Stick Output and Adaptive Filter
Output in the Presence of Motion with $\sigma_{in}=0$; Subject A.
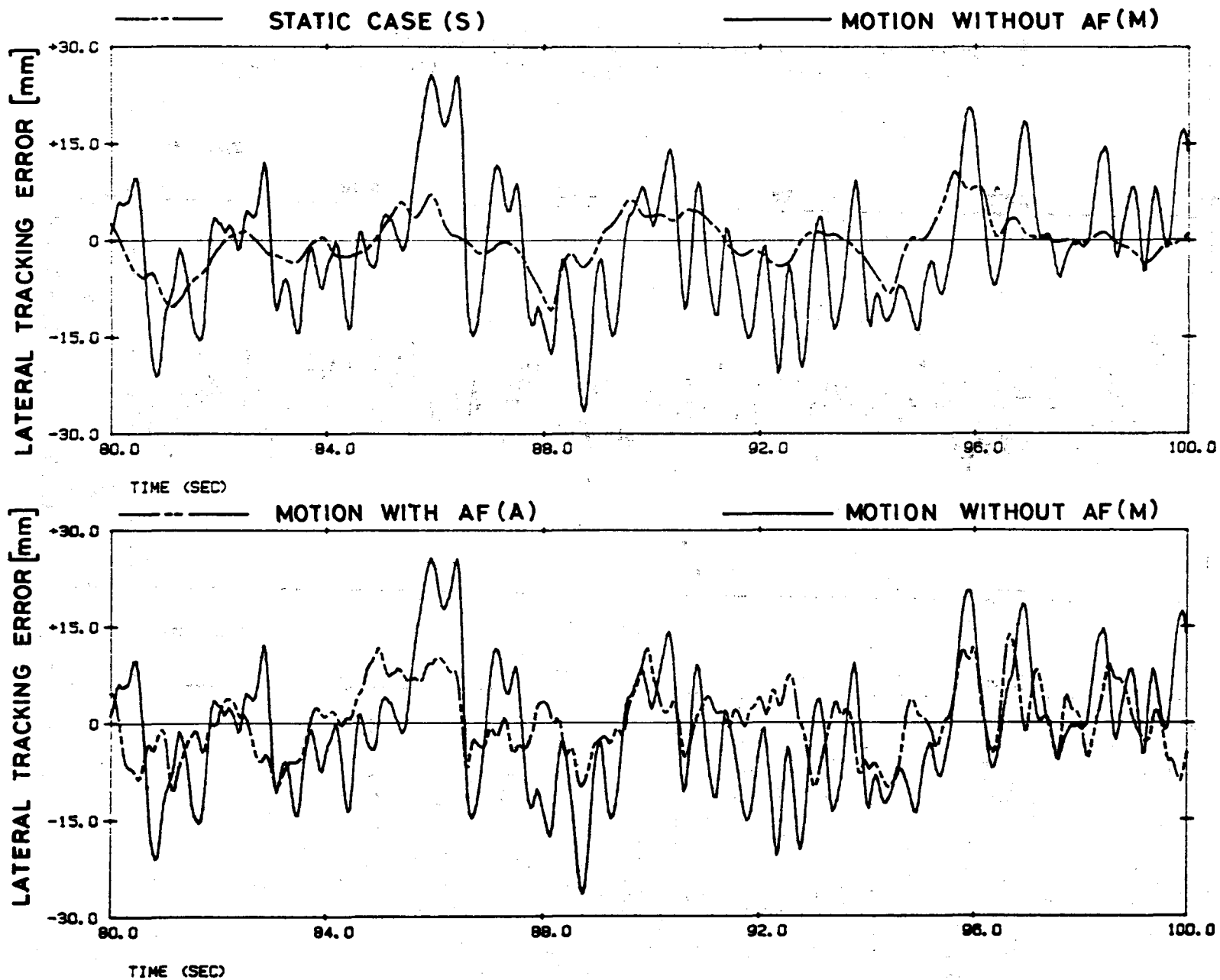
Figure 9. Time Histories of the Tracking Error for the Pursuit Task for Cases S,M and A with σ_{in} =15.5 mm; Subject A.

CONF	SYMBOL	σ_{in} [mm]	K_P
I̱	--▽---	7.8	0.022
I̱I̱	--+---	15.5	0.022
I̱I̱I̱	—○—	31	0.022
I̱V̱	--*--	15.5	0.2

COMPENSATORY TRACKING
SUBJECT A

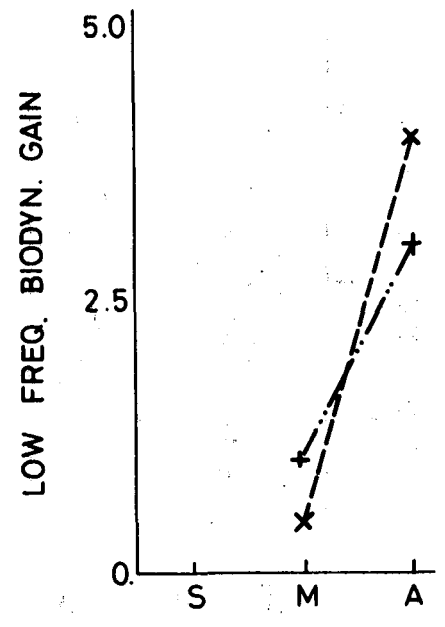|	
S	STATIC
M	MOTION WITHOUT AF
A	MOTION WITH AF
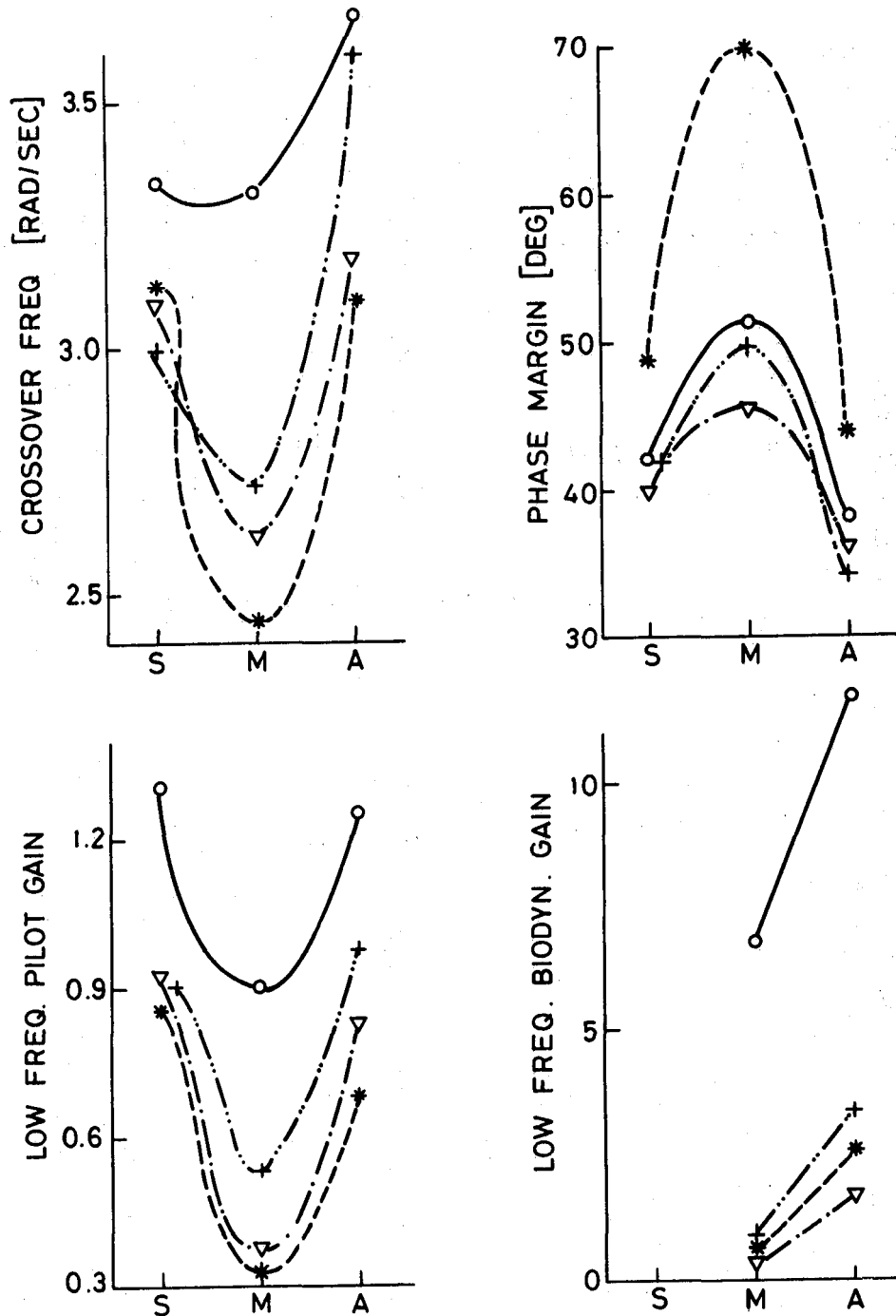
Figure 10. Visual Motor Dynamic Response Properties of the Pilot for the Compensatory Task; Subject A.

717

CONF	SYMBOL	K_P
$\overline{V}$	---·+·---	0.022
$\overline{VI}$	---×---	0.2

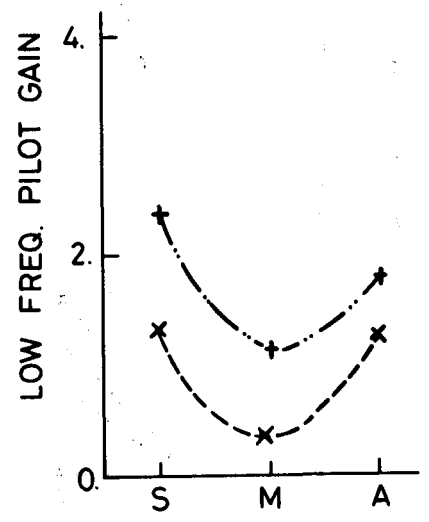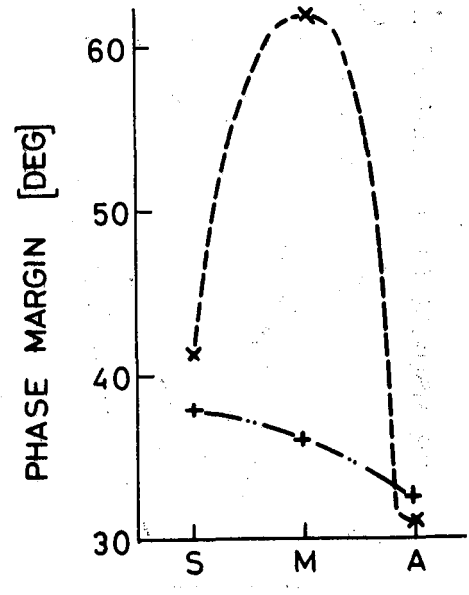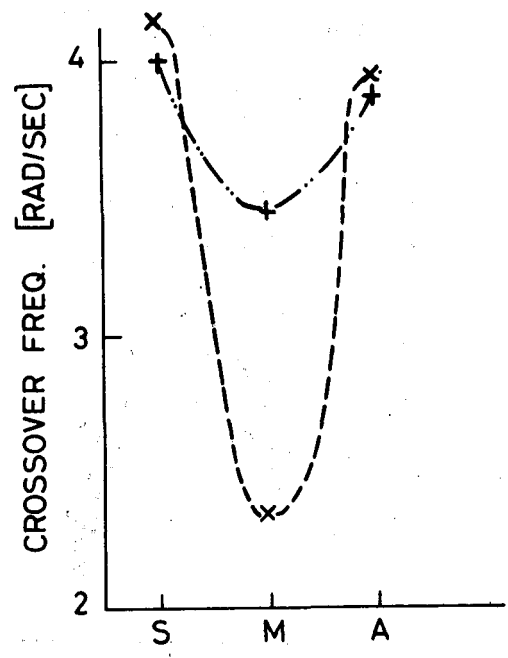|		
S	STATIC	
M	MOTION WITHOUT	AF
A	MOTION WITH	AF

Figure 11. Visual Motor Dynamic Response Properties of the Pilot for the Pursuit Task; Subject A.